

Interactive comment on “Source attribution and process analysis for atmospheric mercury in East China simulated by CMAQ-Hg” by J. Zhu et al.

We thank referees for the positive comments and suggestions. In our response, we have addressed all of the concerns of the reviewers and revised the paper accordingly.

Reply to Referee #1:

The manuscript presents findings from a modeling study of atmospheric mercury deposition in eastern China. This study offers a valuable addition to the scientific literature by providing detailed information on mercury source attribution in a highly polluted region using a fine resolution regional photochemical model. The results will be potentially useful in the prioritization of mercury control measures for different industries in the region. Technical and editorial comments are provided below. I recommend acceptance subject to these minor revisions.

Q: The modeling results are strongly dependent on the mercury chemistry applied in CMAQ. Also, there is considerable uncertainty regarding which mercury transformations actually happen in the atmosphere. Therefore, it would be helpful to provide the details of the chemical mechanism applied in this study.

Re: We quite agree with the referee that atmospheric mercury chemistry is an important uncertain factor in mercury model now since mercury transformations actually happen in the atmosphere and their reaction rate are not known very clearly. As seen in Section 2.1, the chemical mechanism of mercury used in our simulation is CB05 mechanism including mercury gaseous reactions with ozone, OH, H₂O₂ and Cl₂ as described by Lin and Tao (2003). In the future work, we will try to add the mercury reactions with Cl, Br and BrO in CMAQ model to improve the chemical mechanism of mercury.

Q: The authors appear to have not applied the algorithm for bidirectional mercury in

CMAQ but instead included "re-emissions" in the natural mercury emissions. This should be qualitatively discussed.

Re: Yes, we did not apply the algorithm for bidirectional mercury as the CMAQ of version 4.6 we used does not involve this subroutine. Secondary emissions that resulted from deposited mercury transformed to GEM and re-emitted to the atmosphere from soil and water were also considered as described in Shetty et al. (2008).

Q: The basis for the mercury speciation in the anthropogenic source categories should be discussed as this has a strong influence on the predicted impacts. For example, CEM is mostly GEM and thus affects GEM concentrations but has little effect on deposition, whereas IND has a strong effect on deposition.

Re: The mercury speciation in the anthropogenic source categories is given in Table 1. Additionally, the speciation characteristics of each source category were discussed briefly in the beginning of each section for source apportionment (Section 3.2.*).

Q: The work of Zhang et al. regarding mercury in the Beijing area is relevant and should be cited (Atmos. Chem. Phys., 13, 10505–10516, 2013).

Re: OK. We have cited this paper in our manuscript.

Q: "Domestic life" is not a common source category; the basis for the sources including in this category needs to be explained.

Re: As we described in Section 2.2, emission from domestic life (DOM) includes waste incineration, domestic coal burning and application of battery and fluorescent lighting.

Q: In Table 1, Figure 1 and elsewhere in the manuscript: yr⁻¹ is not scientific notation, suggest using either a⁻¹ or spell out "year".

Re: Thank you for the comment. We have changed all “yr” in the manuscript to “year”.

Q: How are wildfire emissions of mercury treated? If they are in the natural source category, there should be a non-zero TPM fraction in Table 1. Also, see line 16 on p.10399.

Re: In our simulation, we treat wildfire and biomass burning emission as part of anthropogenic sources with 13.97 Mg/year GEM and 0.42 Mg/year TPM in China area. However, we did not analyze the modeling result about wildfire and biomass burning emission in detail in our manuscript because of the small emission quantity of this category and the uncertainty of spatial distribution from year to year.

Q: Caption for Figure 2 is inaccurate and needs to be re-worded. Clarify the averaging time period used for evaluation of mercury air concentrations

Re: The time period used for evaluation is 2011 and we have added the time in the caption of Figure 2.

Q: p.10393: Line 6: Provide resolution of the parent grid in the nested grid configuration.

Re: We have added the parent grid resolution of 81x81 km² in this sentence.

Q: p. 10395: Line 20: Provide citation for GEOS-Chem results.

Re: We are sorry that the GEOS-Chem results we used have not been published anywhere for citation.

Q: The grammar and style of writing needs to be checked throughout the manuscript. For example, I recommend the following changes. p. 10391: Lines 9-10: Atmospheric mercury is divided into three species according to various physical and chemical properties Line 12: GEM is the predominant form (> 95 %) in atmosphere; it is very stable

Re: We have revised as referee recommended.

Q: p. 10395-10396: Last line: A comparison was made of characteristics of processes influencing atmospheric mercury species in urban and non-urban areas

Re: We have revised as referee recommended.

Q: p. 10399: Line 1: "NAT was still an important contributor to ..." p. 10396: Line 14: "are shown in Fig. 2"

Re: We have revised as referee recommended.

Q: p. 10399: Line 9: "The effect from NAT was decreasing ..." Abstract: Re-phrase "made gain of mercury"

Re: We have revised as referee recommended.

Q: The notes presented above are just some examples. It would be helpful to proofread the entire manuscript.

Re: Thank you for comments before. We have proofread the entire manuscript again and check the grammar and writing style through the manuscript.

Reply to Referee #3:

This is a nice study investigating source contribution and process analysis for atmospheric mercury in a mercury-polluted region using the CMAQ-Hg model with a nested technique. The findings of this study are useful for better understanding and identifying the key factors that significantly affect atmospheric mercury level and behavior in East China. After the following comments are addressed, I recommend that the manuscript be accepted for publication.

General comments

Q: 1) Anthropogenic Hg emissions from countries around China are generally considerably large and apparently were not considered in this study (Fig. 1a). Those

emissions could significantly affect atmospheric Hg level and behavior in China. Thus they could significantly alter modeled results presented in this paper. The potential impact of neglecting those emissions should be discussed in the manuscript.

Re: We have added some uncertainty analysis for underestimate the anthropogenic sources from other countries in Section 3.2.7. It would lead to the underestimate the contribution from out of China. We will improve the accuracy of anthropogenic sources out of China in the future work.

Q: 2) Elemental Hg demonstrates bi-directional mass exchange between air and surface. A bi-directional exchange model is ideal for accurately simulating dry deposition of element Hg. What kind of scheme/model was used to simulate dry deposition in this study? bi-directional or uni-directional? Are obviously different results expected by using a bi-directional exchange model? The manuscript should give a brief description about the dry deposition model used in the study.

Re: As the CMAQ of version 4.6 of we used does not involve the algorithm for bi-directional mercury. Dry deposition velocity of mercury is calculated by MCIP combined with meteorological condition and the category of land use. Secondary emissions that resulted from deposited mercury transformed to GEM and re-emitted to the atmosphere from soil and water were considered in natural sources as described in Shetty et al. (2008).

Q: 3) GEOS-Chem model generally has much coarser spatial and temporal resolutions than CMAQ-Hg. What are the spatial and temporal resolutions of GEOS-Chem output that were used in this study? If they are coarser than those in CMAQ, how were the GEOS-Chem output processed and adapted to the resolutions employed in CMAQ-Hg simulations?

Re: GEOS-CHEM output we used with spatial resolution of $4^{\circ} \times 4.5^{\circ}$ and temporal resolution of one hour. The output from GEOS-CHEM can be used as the boundary condition for CMAQ with interpolation. However, the coarser resolution will lead to uncertainty for CMAQ modeling results.

Q: 4) In section 3.2, the manuscript presents many numbers and points, but doesn't give sufficient and specific figure citations to support them. It is really difficult for readers to figure them out.

Re: Figure 4 and Figure 5 are used to support section 3.2. Because there are too many categories of emission sources to be compared, it is difficult to express all information in one or two figures and also we cannot show too many figures due to the limited space available for publication.

Technical comments

Q: P10390 L5: "run with nested grid resolution of 27km" to "run with a nested domains"

Re: We have revised as referee recommended.

Q: L10: "regard" to "regarded"

Re: We have revised as referee recommended.

Q: L13: "86.7" to "86.7%"

Re: We have revised as referee recommended.

Q: L24: "7.3" to "7.3 ngm-3"

Re: We have revised as referee recommended.

Q: P10391 L3: Majority of natural emission is element Hg which is chemically inactive.

Why is it more significantly than anthropogenic emission to influence CHEM and AERO?

Re: CHEM and AERO indicate the transform from GEM to GOM and PBM. As GEM from natural emission is larger than that from anthropogenic emission, natural

emission influence CHEM and AERO more.

Q: P10392 L27: "to simulate of regional" to "to simulate regional".

Re: We have revised as referee recommended.

Q: P10393 L8: "with grid resolution of 27x27 km²" to "with a grid resolution of 27 km".

Re: We think "grid resolution of 27x27 km²" is more accurate.

Q: P10395 L16: "comprises" to "covers"

Re: We have revised as referee recommended.

Q: P10396 L7: "natural emissions (NAT) excluded", reword this sentence.

Re: We have reworded this sentence.

Q: P10397 L15: What are time frames and monitoring frequencies of observations?

Re: The time frames and other detail information of observations were summarized in Zhu et al. (2012) and Zhu et al. (2014).

Q: L24: What are specific unexpected complexity for emission and meteorological condition? why?

Re: As the measurement in Pudong last for one month, some sudden emission (without consideration in our emission inventory) during this time frame will affect the averaged condition much. This will lead to the difference between our simulation result and observation.

Q: P10398 L13: PBM concentrations was significantly underestimated as well (by 60%). Why is less precipitation predicted the only reason that caused the underestimation?

Re: We agreed with referee. Less PBM concentration predicted is another reason that

caused the underestimation of wet deposition in Nanjing. We have added this reason in that sentence.

Q: P10403 L17: This sentence is confusing. Reword it.

Re: We have reworded it.

Q: L19: "a factor of >5 larger than" is confusing. Change it.

Re: We have changed it.

Q: P10404 L8: It looks like EMIS and DDEP, instead of EMIS and VDIF, were also the dominant processes. Please check it.

Re: We have checked it again. This sentence talked about EMIS and VDIF and next sentence focused on DDEP.

Q: L18: How are diurnal profiles calculated? Averaged all over non-urban grid cells for a year? A brief description should be added.

Re: Yes, we calculated diurnal profiles by averaged all over urban or non-urban grid cells for a year. We have revised that sentence.

Q: P10416 : label error in figure caption.

Re: We have revised it.

Q: P10421 : add x axis title

Re: We have added the title.

1 **Source attribution and process analysis for atmospheric mercury in**
2 **East China simulated by CMAQ-Hg**

3
4 Jialei Zhu¹, Tijian Wang¹, Johannes Bieser^{2,3}, Volker Matthias²

5 1. School of Atmospheric Sciences, Nanjing University, Nanjing 210093, China

6 2. Institute of Coastal Research, Helmholtz-Zentrum Geesthacht, Max-Planck-Str. 1,
7 21502, Geesthacht, Germany

8 3. National aeronautics and space research center (DRL), Oberpfaffenhofen, 82234,
9 Weßling, Germany

10 Correspondence to: Tijian Wang (tjwang@nju.edu.cn)

11
12 **Abstract**

13 The contribution from different emission sources and atmospheric processes to
14 gaseous elemental mercury (GEM), gaseous oxidized mercury (GOM), particulate
15 bound mercury (PBM) and mercury deposition in East China were quantified using
16 the Community Multi-scale Air Quality (CMAQ-Hg) modeling system run with a
17 nested domain. Natural source (NAT) and six categories of anthropogenic mercury
18 sources (ANTH) including cement production (CEM), domestic life (DOM),
19 industrial boilers (IND), metal production (MET), coal-fired power plants (PP) and
20 traffic (TRA) were considered for source apportionment. NAT was responsible for
21 36.6% of annual averaged GEM concentration which was regarded as the most
22 important source for GEM in spite of obvious seasonal variation. Among ANTH, the
23 influence of MET and PP on GEM were most evident especially in winter. ANTH
24 dominated the variations of GOM and PBM concentration with a contribution of
25 86.7% and 79.1% respectively. Among ANTH, IND was the largest contributor for
26 GOM (57.5%) and PBM (34.4%) so that most mercury deposition came from IND.
27 The effect of mercury emitted from out of China was indicated by >30% contribution

28 to GEM concentration and wet deposition. The contribution from nine processes
29 consisting of emissions (EMIS), gas-phase chemical production/loss (CHEM),
30 horizontal advection (HADV), vertical advection (ZADV), horizontal advection
31 (HDIF), vertical diffusion (VDIF), dry deposition (DDEP), cloud processes (CLDS)
32 and aerosol processes (AERO) were calculated for processes analysis with their
33 comparison in urban and non-urban regions of Yangtze River Delta (YRD). EMIS and
34 VDIF affected surface GEM and PBM concentration most and tended to compensate
35 each other all the time in both urban and non-urban areas. However, DDEP was the
36 most important removal process for GOM with 7.3 ng m^{-3} and 2.9 ng m^{-3} reduced in
37 the surface of urban and non-urban areas respectively in a whole day. Diurnal profile
38 variation of processes revealed the transportation of GOM from urban area to non-
39 urban area and the importance of CHEM/AERO in higher altitudes which caused
40 diffusion of GOM downwards to non-urban area partly. Most of the anthropogenic
41 mercury transported and diffused away from urban area by HADV and VDIF and
42 increase mercury concentration in non-urban areas by HADV. Natural emissions only
43 influenced CHEM and AERO more significantly than anthropogenic. Local emission
44 in the YRD contributed 8.5% more to GEM and ~30% more to GOM and PBM in
45 urban areas compared to non-urban areas.

46

47 1 Introduction

48 Mercury (Hg) pollution in the atmosphere attracts increasing concern globally in
49 view of its neurotoxicity and bioaccumulation in along the food chain posing risks to
50 human health (Schroeder and Munthe, 1998; Rolfhus et al., 2003). Atmospheric
51 mercury is divided into three species according to various physical and chemical
52 properties: gaseous elemental mercury (GEM), gaseous oxidized mercury (GOM) and
53 particulate bound mercury (PBM). GEM is the predominant form (>95%) in
54 atmosphere; it is very stable and well-mixed hemispherically with a long lifetime of

55 0.5~2 years (Selin et al., 2007). In contrast, GOM and PBM will deposit more rapidly
56 downwind of their emission sources via wet or dry deposition since GOM and PBM
57 have significantly higher reactivity, deposition velocities, and water solubility (Lin
58 and Pehkonen, 1999; Lindberg et al., 2002; Keeler et al., 2005). Accordingly, mercury
59 is a multi-scale pollutant able to be transported at local, regional and long scale
60 distances from the sources and mercury emission speciation has a great impact on
61 processes and spatial distribution of mercury in the atmosphere (Bieser et al., 2014;
62 Quan et al., 2009; Voudouri and Kallos, 2007; Pai et al., 1999).

63 Mercury is released into the atmosphere from both natural processes and
64 anthropogenic activities. Natural processes such as evasion from soils, water bodies
65 and vegetation just emit GEM with evident seasonal variation (Shetty et al., 2008).
66 The natural sources will also include re-emission of anthropogenic mercury deposited
67 into the environment previously (Gbor et al., 2006). Mercury emissions from
68 anthropogenic sources are mainly from coal combustion, non-ferrous smelters, waste
69 incineration and mining (Streets, et al., 2009). Anthropogenic mercury emissions in
70 Asia are the highest in the world, accounting for about half of the global total (Pacyna
71 et al. 2010). Especially, China is considered as one of the largest and growing source
72 regions due to its rapid economic and industrial growth along with a coal-dominated
73 energy structure (Wu et al., 2006; Wang et al., 2014). Particularly high emissions of
74 mercury in China result in more elevated mercury concentration and larger mercury
75 deposition than background levels in the world even in remote areas such as the Mt.
76 Gongga area (Fu et al., 2008) and Mt. Changbai (Wan et al., 2009). Much more
77 serious atmospheric mercury pollution was detected in Chinese urban sites where total
78 gaseous mercury (TGM) concentrations were a factor of 3~5 higher than those
79 observed in rural areas (Zhu et al., 2012; Chen et al., 2013; Feng et al., 2004, Zhang et
80 al., 2013). Therefore, improving the understanding of the source-receptor
81 relationships for mercury and providing valuable information on mercury transport,

82 deposition and chemistry within China are urgently needed. Detailed quantitative
83 assessments of the contribution of mercury sources help to determine effective
84 mercury emission control strategies.

85 Previous publications provided contribution estimates from selected emission
86 sources mostly in the United States (Seigneur et al., 2004; Selin and Jacob, 2008; Lin
87 et al., 2012) and the Great Lakes (Cohen et al., 2004; Holloway et al., 2012) using
88 global and regional chemical transport models. Many studies for Asia focus on the
89 mercury mass outflow caused by the total emission in Asia and its contribution to long
90 range transport (Pan et al., 2010; Lin et al., 2010). Limited source apportionment of
91 mercury pollution in China has been studied by Wang et al. (2014) distinguishing four
92 emission sectors using a global model (GEOS-Chem) in coarse spatial resolution. In
93 addition, few studies focus on diagnostic and process analysis for atmospheric
94 mercury pollution formation and identification of the dominant atmospheric processes
95 for mercury. The mercury version of US EPA's Community Multi-scale Air Quality
96 (CMAQ-Hg) modeling system (Bullock and Brehme, 2002) was widely used to
97 simulate regional atmospheric mercury pollution. Process analysis (PA) embedded in
98 CMAQ can be applied to investigate the relative contribution of the individual
99 processes on simulated concentration. The performance of CMAQ-Hg model in
100 simulating mercury has been evaluated against mercury concentration and deposition
101 measured on surface mostly in US (Holloway et al., 2012; Bullock et al., 2008, 2009;
102 Gbor et al., 2006, 2007).

103 In this paper, the temporal and spatial distribution of atmospheric mercury and its
104 deposition in 2011 were simulated on a nested domain over East China with grid
105 resolution of 27x27 km² and parent grid resolution of 81x81 km² using CMAQ-Hg.
106 The model results were compared to available monitoring data. Seasonal
107 contributions of all types of mercury emission sources, including natural emissions,
108 cement plants, domestic coal burning, industrial boilers, metal productions, power

109 plants and traffic emissions, to atmospheric mercury concentration and deposition
110 were quantified. The process analysis for atmospheric mercury concentration was
111 used for select urban and non-urban areas. The influence of physical and chemical
112 processes on mercury concentration was examined. This study provides a detailed
113 model study on source apportionment and process analysis of atmospheric mercury in
114 East China.

115

116 **2 Methods**

117 **2.1 Model descriptions**

118 The model used in this study was based on CMAQ v4.6 which has been modified
119 by Bullock and Brehme (2002) and Gbor et al. (2006) to include chemistry, transport
120 and deposition of GEM, GOM and PBM. The model was configured to use the
121 Carbon Bond 5 (CB05) gaseous phase chemistry mechanism (Sarvar et al., 2008) with
122 Euler Backward Iterative (EBI) solver and the AERO4 aerosol mechanism
123 (Binkowski and Roselle, 2002). The CB05 mechanism used here included mercury
124 gaseous reactions with ozone, OH, H₂O₂ and Cl₂ as described by Lin and Tao (2003).
125 The meteorological fields used in CMAQ-Hg were provided by the Weather Research
126 and Forecasting (WRF v3.2) Model. Meteorology-Chemistry Interface Processor
127 (MCIP v3.6) processed the WRF outputs to the CMAQ-Hg model-ready format and
128 dry deposition velocities of GEM and GOM were calculated. The process analysis
129 (PA) technique is an advanced diagnostic method implemented in CMAQ. It provides
130 hourly integrated process rates to quantify the changes in concentration from each of
131 the scientific processes in the mass conservation equations being solved for each
132 mercury species. During this simulation, the contributions from following physical
133 and chemical processes were calculated: emissions of mercury species (EMIS), net
134 gas-phase chemical production/loss (CHEM), horizontal advection (HADV), vertical
135 advection (ZADV), horizontal diffusion (HDIF), vertical diffusion (VDIF), dry

136 deposition (DDEP), cloud processes (CLDS, including cloud attenuation of photolytic
137 rates, convective and non-convective mixing and scavenging by clouds, aqueous-
138 phase chemistry, and wet deposition), aerosol processes (AERO, including
139 thermodynamic equilibrium and dynamics such as homogeneous nucleation,
140 condensation/evaporation, and coagulation) (Liu and Zhang, 2013).

141

142 **2.2 Emission inventory**

143 Both anthropogenic and natural emission inventories of mercury were employed
144 in our simulation with CMAQ-Hg. Emissions from natural sources (NAT) including
145 vegetation, soil surface and water bodies were based on the estimates by Shetty et al.
146 (2008). GEM is the only species emitted from natural sources. Secondary emissions
147 that resulted from deposited mercury transformed to GEM and re-emitted to the
148 atmosphere from soil and water were also considered. Anthropogenic mercury
149 emissions in China were prepared following the approaches of Wang et al. (2014),
150 which were updated to 2007 (Figure 1a). The inventory data were not consistent with
151 our modeling period, but represented the most updated data at the time when this
152 study was conducted. The monthly variation of anthropogenic sources was based on
153 the monthly energy consumption and product yields published in the Chinese
154 yearbook of provincial diversity. The ratios of three mercury species released were
155 varied according to many factors like coal produced in different provinces, mercury
156 content in coal consumed, different boiler types and removal efficiencies and different
157 combinations of atmosphere pollution control devices (Wang et al., 2014). The total
158 anthropogenic mercury sources (ANTH) in China were classified into six categories
159 for source apportionment: (1) emission from cement production (CEM), (2) emission
160 from domestic life (DOM), which includes waste incineration, domestic coal burning
161 and application of battery and fluorescent lighting, (3) emission from industrial
162 boilers (IND) including boilers used for collective heating in North China during

163 winter, (4) emission from metal production (MET) including zinc smelters, lead
164 smelters, copper smelters, iron production, mercury production and gold production,
165 (5) emissions from coal-fired power plants (PP), which were all treated as large point
166 sources in our simulation, (6) emission from traffic (TRA). Table 1 summarizes the
167 emission inventory for China (land area in the outermost model domain) in 2007. The
168 annual total anthropogenic emissions amount to 638 Mg year⁻¹ which was comparable
169 to natural emissions of 551 Mg year⁻¹. The average speciation of anthropogenic
170 emissions is as follows: (GEM 49.5%, GOM 38.4%, and PBM 12.1%).

171

172 **2.3 Model domain and scenarios**

173 The modeling period covers one year from 20 December 2010 to 31 December
174 2011 including an 11 days spin-up period. Two nested domains were used for CMAQ-
175 Hg model. The first domain (D01, Figure 1a) covers most of China and some other
176 parts of Asia with 85×72 horizontal grid cells at a spatial resolution of 81km×81km.
177 The initial and boundary condition for D01 modeling were extracted from GEOS-
178 Chem global simulation results. The nested domain (D02, Figure 1b) was defined
179 over East China area which is the focus of this study. D02 contains 82×67 horizontal
180 grids with a spatial resolution of 27km×27km. There were 27 vertical layers with a
181 top layer pressure of 100 hPa for both domains. The Yangtze River Delta (YRD)
182 (Figure 1c) is one of the most industrialized and urbanized regions in East China and
183 mercury pollution has become a problem of increasing concern, thus the YRD was
184 chosen for process analysis. Figure 1c showed the land use in the YRD which was
185 divided into three categories of urban, non-urban and water body. A comparison was
186 made of characteristics of processes influencing atmospheric mercury species in urban
187 and non-urban.

188 Nine emission scenarios in China were considered to understand the relative
189 importance of different emission sources to atmospheric mercury concentration and

190 deposition. The base case (BASE) was run with both natural and all anthropogenic
191 sources mentioned above. Seven sensitivity studies (C1~C7) were designed with one
192 of seven source sectors (i.e. NAT, CEM, DOM, IND, MET, PP and TRA) excluded in
193 each study. In addition, the boundary conditions (BC) were set to zero (C8).
194 Subtracting the results of C1~C8 from the BASE case yields an estimate of mercury
195 associated with these mercury sources.

196

197 **3 Results and discussion**

198 **3.1 Model validation**

199 The spatial distribution of annual average concentration and annual total
200 deposition of GEM, GOM and PBM simulated in BASE are shown in Figure 2. The
201 predicted annual average concentration of GEM, GOM and PBM were in the ranges
202 of 1.8~8.4 ng m⁻³, 0.015~1.5 ng m⁻³ and 0.017~1.3 ng m⁻³. On average, GEM
203 constituted 92.8% of the total atmospheric mercury with the contribution going down
204 to a minimum of 58.6% near large anthropogenic sources (Figure 2a). The
205 concentration of GOM and PBM was typically greater at locations of large cities due
206 to the larger anthropogenic emission there and decreased rapidly away from source
207 locations because of their relatively shorter atmospheric lifetimes (Figure 2b,2c). The
208 total mercury deposition was 65.3 μg m⁻² year⁻¹ with 34.3 μg m⁻² year⁻¹ of total dry
209 deposition and 31.0 μg m⁻² year⁻¹ of total wet deposition. The dry deposition of GEM
210 was 4.26 μg m⁻² year⁻¹ on average with the larger deposition in the southern part of
211 D02 due to the larger dry deposition velocity of GEM there (Figure 2d). GOM
212 contributed 28.2 μg m⁻² year⁻¹ to total dry deposition with a range of 2.5~428.4 μg m⁻²
213 year⁻¹, which was the dominant fraction of mercury dry deposition. The distribution
214 of the dry deposition of GOM and PBM resembled the spatial pattern of urban area in
215 East China as a result of high concentration of GOM and PBM there, especially
216 showing the elevated deposition in the eastern (i.e. YRD) and northern part of D02

217 (Figure 2e, 2f). The wet deposition was dominated by PBM (56.5%) followed by
218 GOM (43.4%). The distribution of wet deposition was affected by the spatial pattern
219 of concentration and precipitation (Figure 2h, 2i). The wet deposition of GEM was
220 negligible due to its low solubility in water (Figure 2g).

221 The results from the base case were compared to observations to give a
222 preliminary evaluation of model performance. As long-term mercury measurements in
223 East China are very limited, all available measurement results (listed in Zhu et al.,
224 2012; 2014) in East China were used to assess model skill, of which TGM
225 concentrations were obtained in nine sites, PBM concentrations were obtained in five
226 sites and wet deposition was only observed in Nanjing. The locations of these sites are
227 given in Figure 1b. Although the analysis in the following sections uses the model
228 results for 2011, the same timeframe with observations reported was simulated for
229 model validation. Figure 3 shows the comparison between averaged measurements
230 and CMAQ results during homologous months. Most sites such as Chengshantou (Ci
231 et al., 2011a), Ningbo (Nguyen et al., 2011), Guangzhou (Chen et al., 2013), Jiaying
232 (Wang et al., 2007), Mt. Dinghu (Chen et al., 2013), Chongming (Dou et al., 2013),
233 Nanjing (Zhu et al., 2012) and Yellow Sea (Ci et al., 2011b), the simulated TGM is
234 quite consistent with observations with relative bias of 4%~28% (Figure 3a). In
235 comparison, modeled TGM concentrations in Pudong were ~51% overestimated. The
236 site in Pudong (Friedli et al., 2011) was located at a coastal urban area with less than
237 one month measurement data. The short duration of this measurement and unexpected
238 complex emission and meteorological condition may be responsible for the larger
239 bias. The correlation coefficient between averaged observed and simulated TGM
240 concentration in all sites was 0.85. The model can reproduce the averaged TGM
241 concentration in most areas of East China, but the model results have a smaller
242 variability especially in urban sites like Nanjing where the standard deviation of
243 simulation result was 4.86 ng m^{-3} lower than that observed. This is expected to be the

244 incapability of the model to capture emission plumes and predict the transient peaks
245 observed in urban sites because of the 27 km grid cell resolution and assumption of
246 instantaneous emission dilution in grid cells (Pongprueksa et al., 2008). As seen in
247 Figure 3b, the model results were also comparable to PBM concentration observed in
248 Nanjing (Zhu et al., 2014), Shanghai (Xiu et al., 2009) and Hefei (Wang, 2010). PBM
249 concentration in Nanjing was underestimated by 60% which may be because the
250 location of the observation site in Nanjing is in the central urban area with much
251 higher particle concentration compared to the averaged concentration in the
252 simulation grid cell. The scarcity of mercury deposition measurement in East China
253 limited the evaluation of model performance for mercury deposition. Our model result
254 agrees reasonably well with mercury wet deposition measurement result in Nanjing
255 site during 9 months in 2011 (Zhu et al., 2014) with $6.3\mu\text{g m}^{-2}$ underestimated which
256 was caused by 232.8mm (21.8% to total) less precipitation and less PBM
257 concentration in urban area predicted. Overall, our simulation did well in reflecting
258 the levels and deposition of atmospheric mercury in East China and it is suitable for
259 further analysis of source apportionment.

260

261 **3.2 Source apportionment**

262 **3.2.1 Natural Sources (NAT)**

263 Figure 4 and Figure 5 summarize annual and seasonal relative contribution of
264 different source sectors to atmospheric mercury concentration and deposition in East
265 China (land area in D02). Annual total mercury emissions from natural sources were
266 close to those from anthropogenic sources. Because all natural emissions are in the
267 form of GEM, this sector is responsible for 63.6% of the total annual GEM emission
268 in China. The result was that natural sources are the largest contributor to atmospheric
269 GEM concentration (36.6% in annual average). Due to significant seasonal variation
270 of GEM emission from NAT, the contribution from NAT to GEM varied between

271 52.2% in summer and 15.0% in winter. NAT was much more important for GEM
272 concentration in summer with a factor of 3.3 to the contribution from ANTH (15.9%).
273 Though GEM was not the key species for mercury deposition, NAT was still an
274 important contribution to wet and dry deposition in summer with 28.5% and 24.3%
275 respectively. That was because of higher emission quantity of NAT and the increased
276 photochemical activities in summer that led to a greater degree of GEM oxidation to
277 GOM and transformation to PBM, which contributed 15.7% of GOM and 24.2% of
278 PBM in summer. In contrast, NAT contributes little to GOM concentration (0.2%),
279 PBM concentration (0.3%) and deposition (2.4% to wet deposition and 1.7% to dry
280 deposition) in winter. Therefore, during winter, ANTH had a much larger impact on
281 atmospheric mercury concentration and deposition. The effect from NAT was
282 decreasing from south to north in mainland of D02, correlating with air temperature.
283 There was no obvious difference between the quantities contributed from NAT to
284 urban and rural areas but the relative contribution to urban areas was lower due to
285 higher emissions and thus concentration and deposition in urban areas.

286

287 3.2.2 Cement production (CEM)

288 In 2011, anthropogenic sources emitted 638 Mg of mercury which was a little
289 more than that from natural sources (551 Mg year⁻¹). However, unlike natural sources,
290 mercury from ANTH includes GEM, GOM and PBM. The quantity and speciation of
291 mercury released from six anthropogenic source categories were quite different. This
292 leads to different impacts on the spatial and temporal distribution of atmospheric
293 mercury concentration and deposition.

294 Total mercury emission from CEM is responsible for 13.5% of the total
295 anthropogenic emissions and ~80% of the mercury from CEM was in the form of
296 GEM. CEM contributed 6.6% to the total annual GEM concentration which was
297 23.9% of the total contribution from all anthropogenic sources. The impact on GOM

298 and PBM concentration from CEM was much lower than that of most other
299 anthropogenic sources. As GEM had little impact on mercury deposition, CEM
300 changed wet and dry deposition by only 4.0% and 5.1% respectively. The seasonal
301 variation of the contribution from CEM was negligible because of the production of
302 cement was relatively constant over the whole year. CEM affected the GEM
303 concentration in the eastern coastal area most evidently with up to 20% because of the
304 large emissions from cement plants in the Shandong, Jiangsu and Zhejiang provinces
305 which are responsible for ~26% of the total emissions from CEM in China.

306

307 **3.2.3 Industrial boilers (IND)**

308 Emissions of total mercury from IND made up 32.9% of all anthropogenic
309 emissions in China. Thus, it is the most important anthropogenic source. Moreover,
310 70.8% of the total mercury emitted from IND was GOM which makes up 60.8% of
311 the total GOM emissions in China. Moreover, IND was also the largest source of
312 PBM in China. Owing to the large quantity of GOM and PBM which can deposit near
313 the emission sources through dry and wet deposition, IND makes the largest
314 contribution to mercury deposition with 22.3% and 43.6% to annual wet and dry
315 deposition corresponding to 57.5% and 34.4% contribution to annual averaged GOM
316 and PBM concentration. Especially in winter, IND dominated the GOM concentration
317 and mercury dry deposition with the contribution reaching 73.3% and 63.9%
318 respectively as a result of large-scale collective heating in northern China. The
319 measurement by Zhang et al. (2013) also indicated the boilers play an important role
320 in the elevation mercury concentration in winter of rural Beijing.

321

322 **3.2.4 Power plants (PP)**

323 Emissions from PP were another important sector and they were treated as point
324 sources in the model. GEM and GOM are the main species emitted from PP with a

325 percentage of 68.1% and 30.8% and, in contrast, with only 1.1% of PBM. PP was the
326 smallest contributor (2.5%) to PBM. However, PP was the second largest contributor
327 to GEM and GOM concentration (7.1% and 9.6% respectively) among all
328 anthropogenic sources, although its contribution to GOM concentration was much
329 lower than the largest GOM sources of IND. Emissions from PP were responsible for
330 5.5% and 9.8% of wet and dry deposition which resulted from significant impact on
331 GOM concentration. There were many larger coal-fired power plants with capacities
332 larger than 1000 MW concentrating in the YRD. Because of this, obviously higher
333 emission intensity from PP led to a much higher influence to atmospheric mercury
334 pollution in the YRD with an annual averaged contribution to TGM of up to 1 ng m^{-3}
335 (>20%).

336

337 **3.2.5 Metal production (MET)**

338 MET was the largest anthropogenic source of GEM accounting for 31.8% of the
339 anthropogenically emitted GEM. As this sector includes manufacturers and smelters
340 of various iron and non-iron metals, the content of mercury from MET varied greatly
341 depending on production process and the mercury content in raw materials. The
342 speciation factors ranged from 65% to 89% for GEM, 6% to 30% for GOM, and 0%
343 to 17% for PBM. Overall, MET contributed 8.4%, 8.2% and 5.0% to GEM, GOM and
344 PBM concentration and was responsible for 4.7% and 7.2% of the annual wet and dry
345 deposition in East China respectively. Although MET was distributed widely in East
346 China, the effects of emissions from MET were greatest in Shaanxi Province due to
347 high mercury concentrations in zinc ore and some small scale plants with poor
348 mercury control devices (Wu et al., 2012).

349

350 **3.2.6 Domestic life (DOM) and traffic emission (TRA)**

351 Emissions from DOM (6.3%) and TRA (4.4%) were the small fraction of

352 anthropogenic sources. They both hardly affected GEM concentration with a
353 contribution of less than 1% and had little influence on GOM concentration (4.4%
354 from DOM and 1.8% from TRA). However, over 50% of total PBM emission came
355 from DOM and TRA and they increased the annual averaged PBM concentration by
356 24.4% and 8.0% respectively. As PBM was the main component in mercury wet
357 deposition, DOM was the most important anthropogenic contributor (9.1%) to wet
358 deposition except IND (22.3%). In contrast, DOM and TRA were the two smallest
359 contributors to mercury dry deposition with the proportion of 4.8% and 1.9% because
360 GOM was the dominant contributor to mercury dry deposition. The distribution of
361 emissions from TRA was very heterogeneous with the majority emitted in large cities.
362 In spite of the lower total emissions from TRA, the impacts on PBM concentration
363 and deposition were much higher in and around the province capitals and other large
364 cities by a factor of 2~20 compared to rural areas.

365

366 **3.2.7 Long-range transport (BC)**

367 The impacts of boundary conditions (BC) were also significant for mercury
368 pollution in East China, which indicates the contribution of mercury emission from
369 other source regions. GEM can be transported far beyond the regions where it is
370 emitted and it is hardly deposited. Therefore, GEM in the global mercury pool
371 affected the concentration in China evidently suggested by our simulation result with
372 up to 34.3% annual averaged GEM concentration from BC. However, BC have little
373 effect on GOM concentration with a contribution of only 8.6% because of its
374 relatively short lifetime. The contribution to GEM concentration from BC was largest
375 in winter while the contribution was least to GOM concentration then because of
376 relatively weaker emissions of GEM and stronger emission of GOM in China during
377 winter. BC influenced the annual averaged PBM concentration by 13.3% due to the
378 low dry deposition velocity of fine size PBM. As PBM was removed mainly by wet

379 deposition, BC contributed 32.3% to annual wet deposition of mercury in China. In
380 comparison, only 15.4% of annual dry deposition was linked to BC owing to the small
381 contribution to GOM. Lin et al. (2012) estimated that 89.1% of mercury dry
382 deposition and 93.2% of mercury wet deposition in contiguous US regions are caused
383 by global sources, which is much higher than that ratio estimated for East China in
384 this study. One of the reasons for this is the much higher local anthropogenic emission
385 of mercury in China. Moreover, the anthropogenic sources out of China were not
386 defined accurately. The underestimate of emission sources from other countries would
387 lead to less contribution from BC to East China.

388

389 3.3 Process analysis

390 Figure 2 depicts the simulated concentration and deposition of mercury species
391 during 2011 in East China, which indicated that the Yangtze River Delta (YRD) is one
392 of most polluted areas with high mercury concentration and deposition. Also, the
393 YRD is one of the most active areas of human activity in China. Therefore, the YRD
394 area which is shown in Figure 1c was chosen to study the influence of each physical
395 and chemical process implemented in CMAQ on atmospheric mercury. The area was
396 divided into urban, non-urban and water body depends on the predominant land use.
397 The area with urban coefficient of land use more than 10% was defined as urban area
398 in this study. Comparisons of the contribution of each process to urban and non-urban
399 mercury concentrations were studied.

400

401 3.3.1 Controlling processes

402 The annual averaged diurnal variations of the contribution from nine processes
403 which included horizontal advection (HADV), vertical advection (ZADV), horizontal
404 diffusion (HDIF), vertical diffusion (VDIF), emissions (EMIS), dry deposition
405 (DDEP), cloud physics and scavenging (CLDS) and gas and aerosol phase chemistry

406 (CHEM/AERO) to the concentration of GEM, GOM and PBM in the near-surface
407 layer (the first layer in model which was about 50m) in urban and non-urban areas of
408 the YRD are shown in Figure 6. The results indicate that two major processes
409 dominate surface GEM concentration, namely EMIS and VDIF and their
410 contributions were comparable in urban and non-urban area (Figure 6a). The
411 contributions of EMIS and VDIF to the change of GEM concentration were
412 noticeably temporally variable with much higher values during mid-day. Their
413 contribution in midnight were >5 times larger than those at night and they tended to
414 compensate each other all of the time. The effect of EMIS extended gradually in
415 daytime along with the increase of temperature and solar radiation which led to higher
416 emission from NAT. Anthropogenic activity and production are more active during
417 day time which raised the emissions of mercury, especially in urban area. EMIS was
418 the only processes with a positive contribution to GEM concentration in urban areas
419 with annual average of $1.26 \text{ ng m}^{-3} \text{ h}^{-1}$ and other processes all played the opposite
420 role. However, HADV and ZADV could contribute to both gain and loss of GEM in
421 non-urban area throughout the day. Advection processes had more significant
422 influence on surface GEM concentration during the evening and early morning in
423 both urban and non-urban areas but ZADV had the opposite effect with a positive
424 influence in non-urban and a negative in urban areas at night possibly because of the
425 strong heat island circulation. Processes of DDEP and CLDS made small
426 contributions to the loss of GEM. On average, they reduced the concentration of GEM
427 by about 0.8 ng m^{-3} per day in urban and non-urban areas.

428 Unlike GEM, the contributions from different processes on surface GOM and
429 PBM concentrations were much lower in non-urban than that in urban areas due to
430 lower emissions of GOM and PBM in non-urban areas (Figure 6b, 6c). EMIS and
431 VDIF were also the dominant processes to change surface GOM and PBM
432 concentrations similar to GEM. However, DDEP and CLDS were two additional

433 dominant processes influencing GOM and PBM because of higher dry deposition
434 velocity and reactivity of GOM and PBM. Particularly for GOM, DDEP was the most
435 important removal process with the surface concentration of 7.3 ng m^{-3} and 2.9 ng m^{-3}
436 reduced in urban and non-urban area respectively in a whole day. Local dry deposition
437 of GOM was about 48% of local emissions in urban areas while that in non-urban
438 areas was 42% larger than local emissions which was affected by the emissions from
439 nearby urban areas. In addition, VDIF could contribute to gain of surface GOM in
440 non-urban area in most hours, which indicated higher GOM concentrations in the free
441 troposphere. Figure 7 displays annual averaged diurnal profiles of the variation of
442 HADV, VDIF, CHEM and AERO below 2 km. HADV played almost opposite roles in
443 changing GOM concentration within the boundary layer in urban and non-urban areas
444 (Figure 7a, b), but the trend of temporal variation and magnitude of contribution were
445 about the same. It further indicated the transport of GOM from urban to non-urban
446 areas which was the main source of GOM in upper air of non-urban areas. The
447 contribution of VDIF to the GOM concentration is displayed in Figure 7c. More
448 horizontally advected GOM aloft was mixed downwards to ground levels along with
449 the increase of boundary layer height with the largest contribution of $\sim 0.06 \text{ ng m}^{-3} \text{ h}^{-1}$
450 at noon, which was why the contribution from VDIF was positive in the surface layer
451 and negative in higher altitudes. CHEM was another contributor to the accumulation
452 of GOM as well as AERO to PBM in the upper air, though CHEM and AERO seemed
453 to be negligible to change GOM and PBM concentration in the surface layer. Figure
454 7d-7f show that the contributions of CHEM and AERO were much higher in the upper
455 layers than that at surface especially around noon since most of mercury chemical
456 reactions rely on solar radiation. CHEM and AERO are the most important processes
457 to transform GEM to GOM and PBM in the atmosphere. Within 2 km upon non-urban
458 areas, the column concentration of GOM was increased by 41.9 ng m^{-2} owing to the
459 transformation of GEM through CHEM and the column concentration of PBM was

460 enhanced by 29.1 ng m^{-2} through AERO in a whole day. The enhancements of GOM
461 and PBM through CHEM and AERO in urban area was about 13% less than that in
462 non-urban area. A combination of HADV, ZADV, VDIF, DDEP and CLDS tended to
463 cancel out the gain of PBM from EMIS and AERO in urban area. In spite of most
464 decrease from VDIF in urban area, the other four processes also make 21%
465 contribution to remove surface PBM. However, both of HADV and ZADV
466 transported PBM to surface layer in non-urban areas. The strongest increase of surface
467 PBM occurred in the afternoon at 16-18 h due to higher emission rates of DOM and
468 TRA which were the most important source for PBM while most of the decrease
469 occurred in the morning between 9-11 h because the VDIF process was most effective
470 then. In urban areas, the contribution from DDEP to PBM was 20% less than that
471 from CLDS. In comparison, DDEP made 57% more contribution than CLDS to the
472 loss of surface PBM in non-urban areas. The contribution from HDIF was negligible
473 for all of GEM, GOM and PBM concentrations.

474

475 **3.3.2 Impacts of sources on processes**

476 Different mercury emission sources had different influences on processes due to
477 the different distribution and intensity of emission sources. The contributions of
478 natural sources and various anthropogenic sources to GEM processes in urban and
479 non-urban areas of the YRD are compared in Figure 8. Various anthropogenic sources,
480 especially CEM and PP, were the main sources leading to GEM advection out of
481 urban areas with $0.077 \text{ ng m}^{-3} \text{ h}^{-1}$ by HADV while natural sources mainly caused
482 GEM to be horizontally transported away from non-urban areas with $0.021 \text{ ng m}^{-3} \text{ h}^{-1}$
483 (Figure 8a). ANTH made a similar contribution to DDEP and CHEM of GEM in both
484 non-urban and urban areas. In comparison, natural sources affected DDEP and CHEM
485 of GEM >110% more in non-urban than urban areas though emission from NAT in
486 non-urban area only 38% more than that in urban area (Figure 8d, 8e). Conversely,

487 NAT caused comparable loss of GEM by VDIF in both areas and ANTH influenced
488 VDIF of GEM in urban areas much more evidently (Figure 8c). In the YRD,
489 emissions of GEM mostly came from CEM and PP which contributed locally to GEM
490 concentrations with 0.32 and 0.27 ng m⁻³ h⁻¹ in urban areas. More than 80% of the
491 GEM emissions in non-urban areas were emitted by natural sources (Figure 8b).
492 Totally, local emission in the YRD contributed 37.2% to the annual averaged GEM
493 concentration in non-urban and 45.7% to that in urban areas.

494 Local emissions in the YRD were the primary source for GOM and PBM
495 concentration with a contribution of 74.8% (92.9%) to GOM concentration and 44.0%
496 (66.0%) to PBM concentration in non-urban (urban) area respectively. As GOM and
497 PBM were the main constituents of mercury deposition, local emission in the YRD
498 contributed 65.1% (88.7%) to the annual mercury dry deposition and 37.3% (56.2%)
499 to mercury wet deposition in non-urban (urban) of YRD area. Obviously, local
500 emissions have a larger influence on mercury concentration and deposition in urban
501 areas. However, local emissions also were the most important factor for mercury
502 pollution in non-urban areas. Figure 9 and Figure 10 show the contribution from
503 different sources on the various processes of GOM and PBM in two areas. Natural
504 sources only affected CHEM and AERO especially in non-urban areas significantly
505 compared to anthropogenic sources (Figure 9e, 10e). IND was the largest contributor
506 to all processes of GOM except for CHEM (Figure 9) while DOM contributed most to
507 all processes of PBM besides of AERO (Figure 10). All anthropogenic sources
508 increased the outflow of GOM and PBM from urban areas and enhanced the inflow
509 into non-urban areas. Moreover, the quantity of inflow in non-urban areas was
510 directly proportional to the outflow in urban areas which also indicates the influence
511 of urban emissions on mercury pollution in non-urban areas via HADV (Figure 9a,
512 10a). Figure 9c depicts that the effects of PP to VDIF of GOM were opposite to those
513 of other anthropogenic sources. Emissions from PP enhanced the surface GOM

514 concentration by VDIF, which was because the emissions from PP was mostly in the
515 free troposphere and formed a large concentration center there. Most of the GOM in
516 higher altitudes would be diffused to the surface in local urban areas and others would
517 be transported to non-urban areas and then increase surface GOM concentration there
518 by VDIF. Due to the limited emissions of PBM from PP, the influence on VDIF of
519 PBM from PP was negligible (Figure 10c).

520

521 **4. Conclusion**

522 The simulation of atmospheric mercury in East China was conducted using
523 CMAQ-Hg with a grid resolution in a nested domain of 27km to study source
524 apportionment and process analysis. An updated mercury emission inventory for 2007
525 with anthropogenic emission of 638 Mg year⁻¹ in China as well as emissions from
526 natural sources of 551 Mg year⁻¹ was used for this simulation. The base model results
527 were consistent with the measurements of atmospheric mercury including the
528 concentration of TGM and PBM as well as the wet deposition in most sites of East
529 China.

530 Model results for source apportionment showed that natural emissions are the
531 most important source for GEM concentration in East China with a contribution of
532 36.6%. However natural sources were less important in winter than anthropogenic
533 sources due to significant seasonal variation of emissions. Among the anthropogenic
534 sources, metal production (MET) and power plants (PP) were largest contributors to
535 GEM. For GOM and PBM, anthropogenic sources dominated the variation of
536 concentration with a contribution of 86.7% and 79.1% to the annual averaged
537 concentrations. Industrial sources (IND) were responsible for 57.5% of the GOM
538 concentration on average with the highest influence during winter time. IND also
539 contributed significantly to PBM together with domestic sources (DOM) and they
540 accounted for 58.8% of annual averaged PBM. 42.7% and 62.4% of wet and dry

541 deposition of mercury in East China came from anthropogenic sources respectively.
542 Because of the large contribution to GOM and PBM, IND led to the most mercury
543 deposition. Natural sources amounted a quarter of wet and dry deposition in summer
544 owing to higher emissions and the increased photochemical oxidation to GOM and
545 transformation to PBM during this season. The impact of mercury emitted from
546 outside of China was also significant for mercury pollution in East China. This was
547 indicated by a contribution of more than 30% from the model boundary conditions
548 (BC) to GEM concentration and wet deposition.

549 The influence of atmospheric processes on mercury concentration in the near-
550 surface layer was analyzed in urban and non-urban areas of the YRD. Emissions and
551 vertical diffusion affected surface GEM and PBM concentration most and tended to
552 compensate each other all the time in both urban and non-urban areas. However, dry
553 deposition was the most important removal process for GOM with 7.3 ng m^{-3} and 2.9
554 ng m^{-3} deposited in urban and non-urban areas respectively on an average day. The
555 variation of diurnal profiles of different processes (i.e.: HADV, VDIF, CHEM and
556 AERO) inside the planetary boundary layer indicated the transport of mercury from
557 urban to non-urban areas. Moreover, it was found that gas phase and aerosol
558 chemistry (CHEM and AERO) have a large impact on GOM and PBM concentrations
559 inside the free troposphere. The high concentration of GOM aloft in non-urban areas
560 could be diffused downwards by VDIF. Most of anthropogenic sources caused
561 mercury to be transported and diffused away from urban areas by HADV and VDIF
562 and increased the concentration in non-urban areas by HADV. In contrast, emissions
563 from power plants (PP) enhanced surface GOM concentration by VDIF because
564 emission from PP led to a large concentration center in upper air. Natural sources only
565 influenced CHEM and AERO in both areas more significantly than anthropogenic
566 sources. Local emission in the YRD contributed 8.5% more to GEM and ~30% more
567 to GOM and PBM in urban than those in non-urban areas

569 **Acknowledgements**

570 This work was supported by the National Key Basic Research Development
571 Program of China (2014CB441203,2011CB403406), the Specialized Research Fund
572 for the Doctoral Program of Higher Education of China (20110091110010) and a
573 project funded by the Priority Academic Program Development of Jiangsu Higher
574 Education Institutions (PAPD). Thanks to Prof. Shuxiao Wang and Dr. Long Wang
575 from Tsinghua University for providing mercury emission data.

576 **Reference**

- 577 Bieser, J., De Simone, F., Gencarelli, C., Geyer, B., Hedgecock, I., Matthias, V.,
578 Travnikov, O. and Weigelt, A.: A diagnostic evaluation of modeled mercury wet
579 depositions in Europe using atmospheric speciated high-resolution observations,
580 *Environ. Sci. Pollut. Res.*, 21(16), 9995-10012, 2014.
- 581 Binkowski, F. S. and Roselle, S. J.: Models-3 Community Multiscale Air Quality
582 (CMAQ) model aerosol component 1. Model description, *J. Geophys. Res.*, 108,
583 4183–4201, doi:10.1029/2001JD001409, 2003.
- 584 Bullock, O. R. J. and Brehme, K. A.: Atmospheric mercury simulation using the
585 CMAQ model: formulation description and analysis of wet deposition results,
586 *Atmos. Environ.*, 36, 2135–2146, doi:10.1016/S1352-2310(02)00220-0, 2002.
- 587 Bullock, O. R., Atkinson, D., Braverman, T., Civerolo, K., Dastoor, A., Davignon, D.,
588 Ku, J.-Y., Lohman, K., Myers, T. C., Park, R. J., Seigneur, C., Selin, N. E., Sistla,
589 G., and Vijayaraghavan, K.: An analysis of simulated wet deposition of mercury
590 from the North American Mercury Model Intercomparison Study, *J. Geophys.*
591 *Res.*, 114, 1–12, doi:10.1029/2008JD011224, 2009.
- 592 Bullock, O. R., Atkinson, D., Braverman, T., Civerolo, K., Dastoor, A., Davignon, D.,
593 Ku, J.-Y., Lohman, K., Myers, T. C., Park, R. J., Seigneur, C., Selin, N. E., Sistla,
594 G., and Vijayaraghavan, K.: The North American Mercury Model
595 Intercomparison Study (NAMMIS): Study description and model-to-model
596 comparisons, *J. Geophys. Res.*, 113, 1–17, doi:10.1029/2008JD009803, 2008.
- 597 Chen, L., Liu, M., Xu, Z., Fan, R., Tao, J., Chen, D., Zhang, D., Xie, D. and Sun, J.:
598 Variation Trends and Influencing Factors of Total Gaseous Mercury Inthe Pearl
599 River Delta-A Highly Industrialised Region in South Chinainfluenced by
600 Seasonal Monsoons. *Atmos. Environ.*, 77, 757-766, 2013.
- 601 Ci, Z.J., Zhang, X.S., Wang, Z.W. and Niu, Z.C.: Atmospheric gaseous elemental
602 mercury (GEM) over a coastal/rural site downwind of East China: temporal

603 variation and long-range transport. *Atmos. Environ.*, 45, 2480-2487, 2011a.

604 Ci, Z.J., Zhang, X.S., Wang, Z.W., Niu, Z.C., Diao, X.Y. and Wang, S.W.: Distribution
605 and air-sea exchange of mercury (Hg) in the Yellow Sea. *Atmos. Chem. Phys.* 11,
606 2881-2892, 2011b.

607 Cohen, M., Artz, R., Draxler, R., Miller, P., Poissant, L., Niemi, D., Ratté, D.,
608 Deslauriers, M., Duval, R., Laurin, R., Slotnick, J., Nettesheim, T., and
609 McDonald, J.: Modeling the atmospheric transport and deposition of mercury to
610 the Great Lakes, *Environ. Res.*, 95, 247-265, 2004.

611 Dou, H., Wang, S., Wang, L., Zhang, L. and Hao, J.: Characteristics of Total Gaseous
612 Mercury Concentrations at a Rural Site of Yangtze Delta, China. *Environ. Sci.*
613 (in Chinese), 34, 1-7, 2013.

614 Feng, X., Shang, L., Wang, S., Tang, S., and Zheng, W.: Temporal variation of total
615 gaseous mercury in the air of Guiyang, China, *J. Geophys. Res.*, 109, D03303,
616 doi:10.1029/2003JD004159, 2004.

617 Friedli, H.R., Arellano, A.F., Geng, and F., Pan, L.: Measurements of atmospheric
618 mercury in Shanghai during September 2009, *Atmos. Chem. Phys.*, 11, 3781-
619 3788, 2011.

620 Fu, X. W., Feng, X. B., Zhu, W. Z., Wang, S. F., and Lu, J.: Total gaseous mercury
621 concentrations in ambient air in the eastern slope of Mt. Gongga, South-Eastern
622 fringe of the Tibetan plateau. *China. Atmos. Environ.* 42, 970–979, 2008

623 Gbor, P. K., Wen, D., Meng, F., Yang, F., Zhang, B. and Sloan, J. J.: Improved model
624 for mercury emission, transport and deposition, *Atmos. Environ.* 40, 973-983,
625 2006.

626 Gbor, P., Wen, D., Meng, F., Yang, F., and Sloan, J.: Modeling of mercury emission,
627 transport and deposition in North America, *Atmos. Environ.*, 41, 1135–1149,
628 doi:10.1016/j.atmosenv.2006.10.005, 2007.

629 Holloway, T., Viogt, C., Morton, J., Spak, S. N., Rutter, A. P. and Schauer, J. J.: An

630 assessment of atmospheric mercury in the Community Multiscale Air Quality
631 (CMAQ) model at an urban site and a rural site in the Great Lakes Region of
632 North America, *Atmos. Chem. Phys.*, 12, 7117-7133, 2012.

633 Keeler, G. J., Gratz, L. E., and Al-Wali, K.: Long-term Atmospheric Mercury Wet
634 Deposition at Underhill, Vermont, *Ecotoxicology*, 14, 71–83, 2005.

635 Lin, C. J. and Pehkonen, S. O.: The chemistry of atmospheric mercury: A review,
636 *Atmos. Environ.*, 33, 2067–2079, 1999.

637 Lin, C. J., Pan, L., Steets, D. G., Shetty, S. K., Jang, C., Feng, X., Chu, H. W. and Ho,
638 T. C.: Estimating mercury emission outflow from East Asia using CMAQ-Hg,
639 *Atmos. Chem. Phys.*, 10, 1853-1864, 2010.

640 Lin, C. J., Shetty, S. K., Pan, L., Pongprueksa, P., Jang, C. and Chu, H.: Source
641 attribution for mercury deposition in the contiguous United States: Regional
642 difference and seasonal variation, *J. Air Waste Manage*, 62(1), 52-63, 2012.

643 Lin, X. and Tao, Y.: A numerical modelling study on regional mercury budget for
644 eastern North America, *Atmos. Chem. Phys.*, 3, 535-548, 2003.

645 Lindberg, S. E., Brooks, S., Lin, C. J., Scott, K. J., Landis, M. S., Stevens, R. K.,
646 Goodsite, M., and Richter, A.: Dynamic oxidation of gaseous mercury in the
647 arctic troposphere at polar sunrise, *Environ. Sci. Technol.*, 36, 1245–1256,
648 doi:10.1021/es0111941, 2002.

649 Liu, X. and Zhang, Y: Understanding of the formation mechanisms of ozone and
650 particulate matter at a fine scale over the southeastern U.S.: Process analyses and
651 responses to future-year emissions, *Atmos. Environ.*, 74, 259-276, 2013.

652 Nguyen, D., Kim, J., Shim, S. and Zhang, X.: Ground and shipboard measurements of
653 atmospheric gaseous elemental mercury over the Yellow Sea region during
654 2007–2008, *Atmos. Environ.*, 41, 253-260, 2011.

655 Pacyna, E.G., Pacyna, J.M., Sundseth, K., Munthe, J., Kindbom, K., Wilson, S.,
656 Steenhuisen, F., and Maxson, P.: Global emission of mercury to the atmosphere

657 from anthropogenic sources in 2005 and projections to 2020. *Atmospheric*
658 *Environment* 44, 2487-2499, 2010.

659 Pai, P., Karamchandani, P., Seigneur, C. and Allan M.: Sensitivity of simulated
660 atmospheric mercury concentrations and deposition to model input parameters, *J.*
661 *Geophys. Res.*, 104, 13855-13868, 1999.

662 Pan, L., Lin, C. J., Carmichael, G. R., Streets, D. G., Tang, Y., Woo, J. H., Shetty, S.
663 K., Chu, H. W., Ho, T. C., Friedli, H. R. and Feng, X.: Study of atmospheric
664 mercury budget in East Asia using STEM-Hg modeling system, *Sci. Total*
665 *Environ.*, 408, 3277-3291, 2010.

666 Pongprueksa, P., Lin, C. J., Lindberg, S.E., Jang, C., Braverman, T., Russell Bullock
667 Jr., O., Ho, T. C. and Chu, H. W.: Scientific uncertainties in atmospheric mercury
668 models III: boundary and initial conditions, model grid resolution, and Hg(II)
669 reduction mechanism. *Atmos. Environ.*, 42(8), 1828–1845, 2008.

670 Quan, J., Zhang, Q. and Zhang, X.: Emission of Hg from coal consumption in China
671 and its summertime deposition calculated by CMAQ-Hg, *Terr. Atmos. Ocean.*
672 *Sci.*, 20,325-331, 2009.

673 Rolfhus, K.R., Sakamoto, H.E., Cleckner, L.B., Stoor, R.W., Babiarz, C.L., Back,
674 R.C., Manolopoulos, H., Hurley, J.P.: Distribution and fluxes of total and methyl
675 mercury in Lake Superior. *Environ. Sci. and Technol.*, 37, 865–872, 2003.

676 Sarwar, G., Luecken, D., Yarwood, G., Whitten, G. Z., and Carter, W. P. L.: Impact of
677 an Updated Carbon Bond Mechanism on Predictions from the CMAQ Modeling
678 System: Preliminary Assessment, *J. Appl. Meteorol. Clim.*, 47, 3–14,
679 doi:10.1175/2007JAMC1393.1, 2008.

680 Schroeder, W.H., and Munthe, J.: Atmospheric mercury—an overview. *Atmos.*
681 *Environ.* 32, 809–822, 1998.

682 Seigneur, C., Vijayaraghavan, K., Lohman, K., Karamchandani, P., and Scott, C.:
683 Global Source Attribution for Mercury Deposition in the United States, *Environ.*

684 Sci. Technol., 38, 555-569, 2004.

685 Selin, N. E., and Jacob, D. J.: Seasonal and spatial patterns of mercury wet deposition
686 in the United States: constraints on the contribution from North American
687 anthropogenic sources, *Atmos. Environ.*, 42 (21), 5193–5204, 2008.

688 Selin, N. E., Jacob, D. J., Park, R. J., Yantosca, R. M., Strode, S., Jaegle, L., and Jaffe,
689 D.: Chemical cycling and deposition of atmospheric mercury: Global constraints
690 from observations, *J. Geophys. Res.-Atmos.*, 112, D02308,
691 doi:10.1029/2006jd007450, 2007.

692 Shetty, S., Lin, C., Streets, D., and Jang, C.: Model estimate of mercury emission
693 from natural sources in East Asia, 42, 8674-8685, 2008.

694 Streets, D. G., Zhang, Q. and Wu, Y.: Projections of global mercury emissions in
695 2050, *Environ. Sci. Technol.*, 36(8), 2983-2988, 2009.

696 Wan, Q., Feng, X.B., Lu, J.L., Zheng, W., Song, X.J., Li, P., Han, S.J., and Xu, H.:
697 Atmospheric mercury in Changbai Mountain area, northeastern China I: the
698 season distribution pattern of total gaseous mercury and its potential sources.
699 *Environ. Res.* 109, 201–206, 2009.

700 Wang, L., Wang, S., Zhang, L., Wang, Y., Zhang, Y., Nielsen, C., McElroy, M. B. and
701 Hao, J.: Source apportionment of atmospheric mercury pollution in China using
702 the GEOS-Chem model, *Environ. Pollut.*, 190, 166-175, 2014.

703 Wang, Y.: The speciation, levels and potential impacted factors of atmospheric
704 mercury in Hefei, Central China (in Chinese), University of Science and
705 Technology of China, 2010.

706 Wang, S.X., Zhang, L., Wang, L., Wu, Q.R., Wang, F. Y. and Hao, J. M.: A review of
707 atmospheric mercury emissions, pollution and control in China. *Front. Environ.*
708 *Sci. Eng.*, DOI: 10.1007/s11783-014-0673-x, 2014.

709 Wang, Z.W., Chen, Z.S., Duan, N., and Zhang, X.S.: Gaseous elemental mercury
710 concentration in atmosphere at urban and remote sites in China. *J. Environ. Sci.*

711 19, 176–180, 2007.

712 Wu, Q.R., Wang, S.X., Zhang, L., Song, J.X., Yang, H. and Meng, Y.: Update of
713 mercury emissions from China's primary zinc, lead and copper smelters, 2000-
714 2010, *Atmos. Chem. Phys.*, 12, 11153-11163, 2012.

715 Wu, Y., Wang, S., Streets, D. G., Hao, J., Chan, M. and Jiang, J.: Trends in
716 Anthropogenic Mercury Emissions in China from 1995 to 2003. *Environ. Sci.*
717 *Technol.*, 40, 5312-5318, 2006.

718 Xiu, G., Cail, J., Zhang, W., Zhang, D., Bueler, A., Lee, S., Shen, Y., Xu, L., Hunag,
719 X., Zhang, P.: Speciated mercury in size-fractionated particles in Shanghai
720 ambient air. *Atmos. Environ.*, 43, 3145-3154, 2009.

721 Zhang, L., Wang, S. X., Wang, L. and Hao, J. M.: Atmospheric mercury concentration
722 and chemical speciation at a rural site in Beijing, China: implications of mercury
723 emission sources. *Atmos. Chem. Phys.*, 13, 10505–10516, 2013.

724 Zhu, J., Wang, T., Talbot, R., Mao, H., Hall, C. B., Yang, X., Fu, C., Zhuang, B., Li,
725 S., Han, Y. and Huang, X.: Characteristics of atmospheric Total Gaseous
726 Mercury (TGM) observed in urban Nanjing, China. *Atmos. Chem. Phys.*, 12,
727 12103–12118, 2012.

728 Zhu, J., Wang, T., Talbot, R., Mao, H., Yang, X., Fu, C., Sun, J, Zhuang, B., Li, S.,
729 Han, Y. and Xie, M.: Characteristics of atmospheric mercury deposition and size-
730 fractionated particulate mercury in urban Nanjing, China. *Atmos. Chem. Phys.*,
731 12, 2233–2244, 2014.

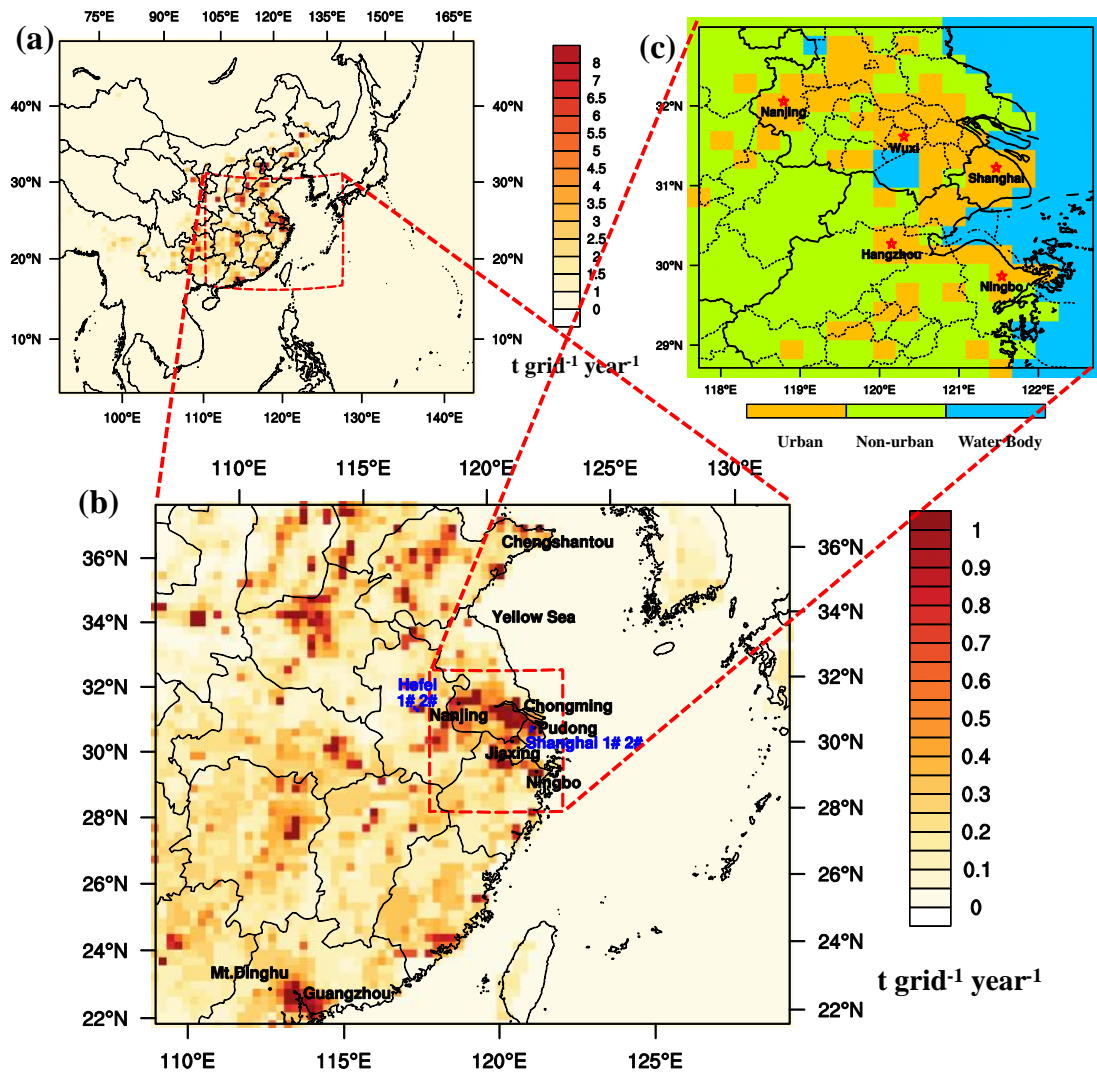
732

733

Table 1 Summary of mercury emissions in the model domain 1

	GEM(Mg/year)	GOM(Mg/year)	TPM(Mg/year)	Total(Mg/year)
Natural	551	0	0	551
Anthropogenic	316	245	77	638
CEM	69.0	12.9	4.3	86.2
DOM	6.4	9.2	24.7	40.3
IND	34.1	149.0	27.2	210.3
MET	100.6	30.1	5.3	136.0
PP	84.2	38.1	1.3	123.6
TRA	8.1	5.9	14.0	28.0
Total	867	245	77	1189

734



735

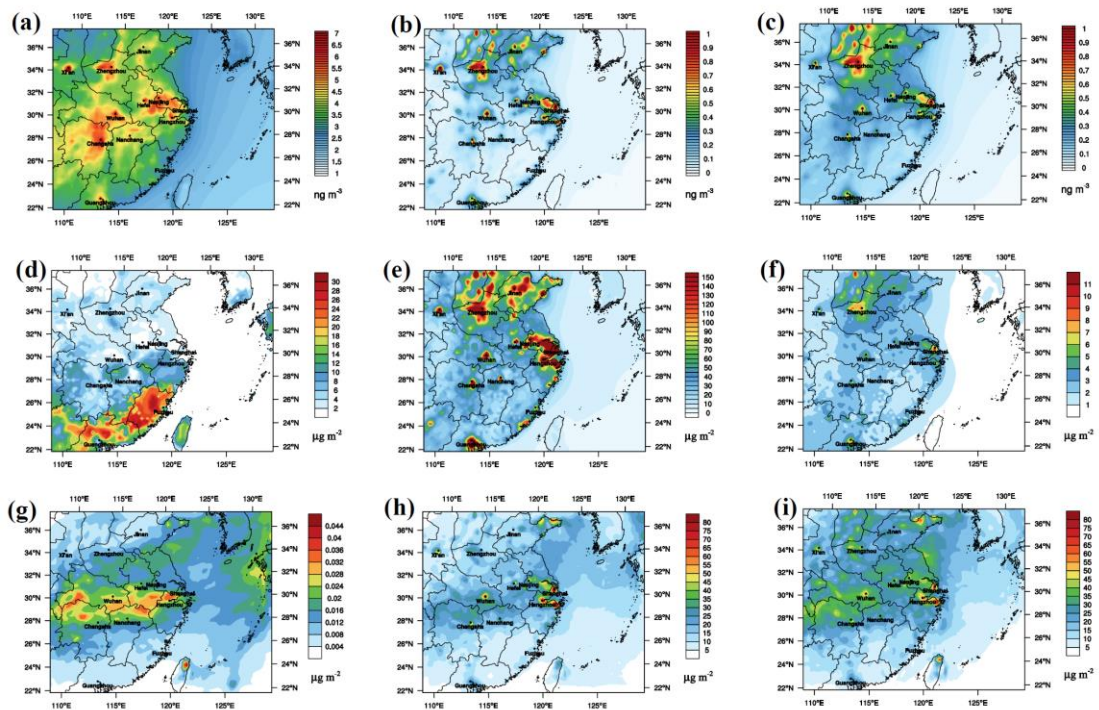
736 Figure 1 Model domain (a) Domain 1 with annual total mercury emission (b) Domain

737 2 with annual total mercury emission (c) Yangtze River Delta (YRD) area with land

738

use category

739



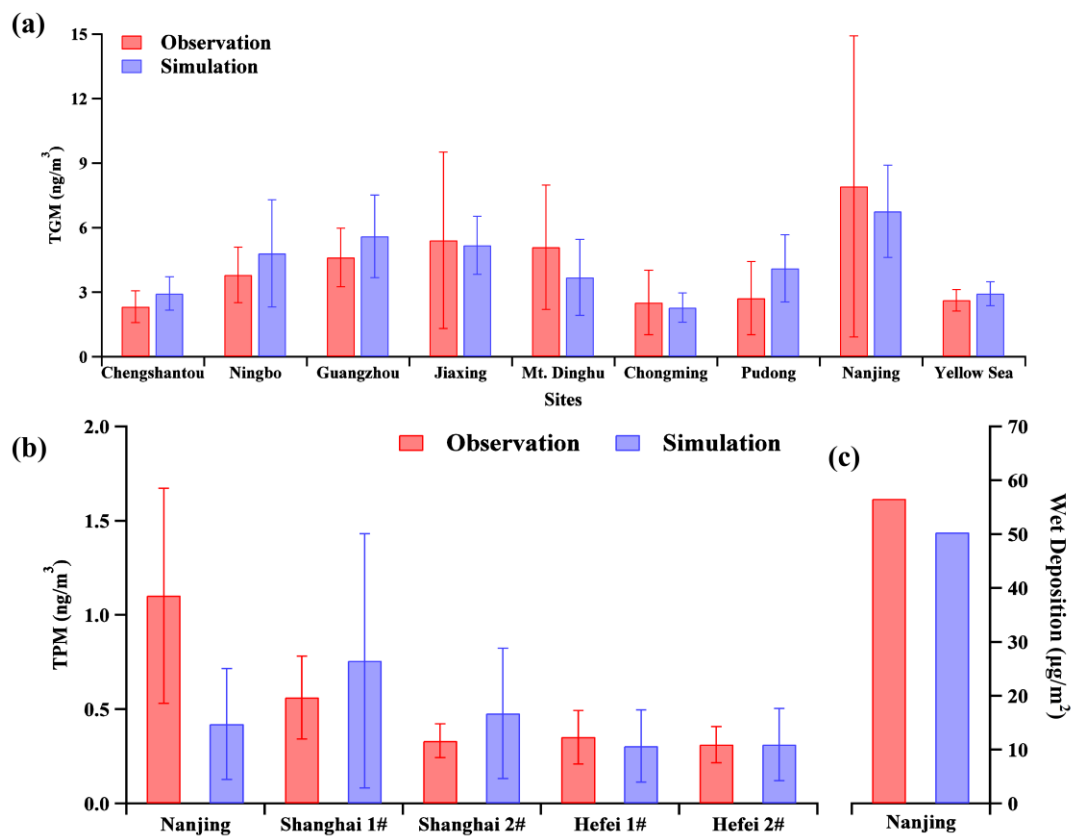
740

741 Figure 2 Simulated annual average concentration of (a) GEM, (b) GOM and (c) PBM,

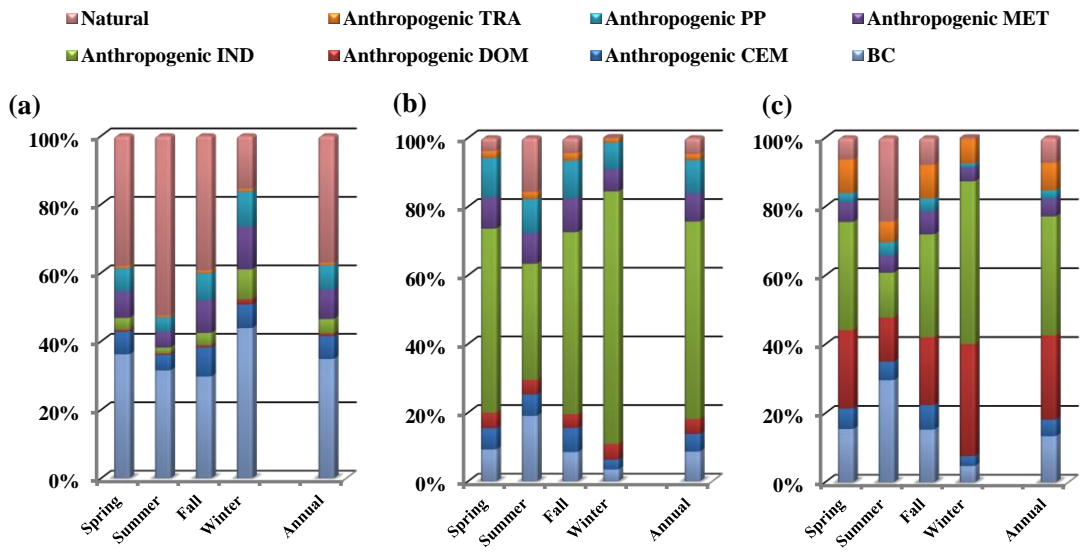
742 annual dry deposition of (d) GEM, (e) GOM and (f) PBM and dry deposition of (g)

743 GEM, (h) GOM and (i) PBM in East China in 2011

744



745
 746 Figure 3 Comparison between simulated results and measurements in sites for (a)
 747 TGM concentration, (b) PBM concentration and (c) wet deposition.
 748

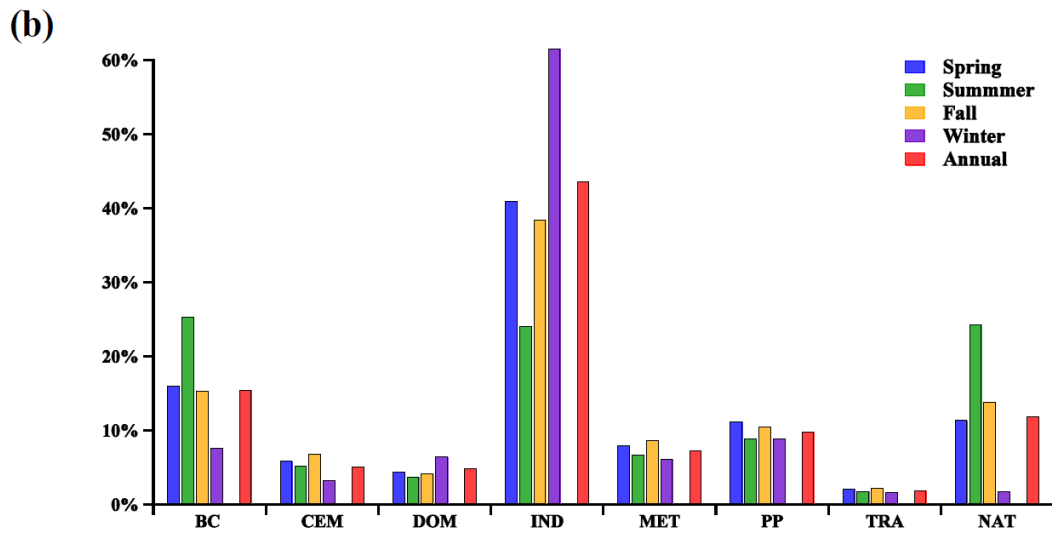
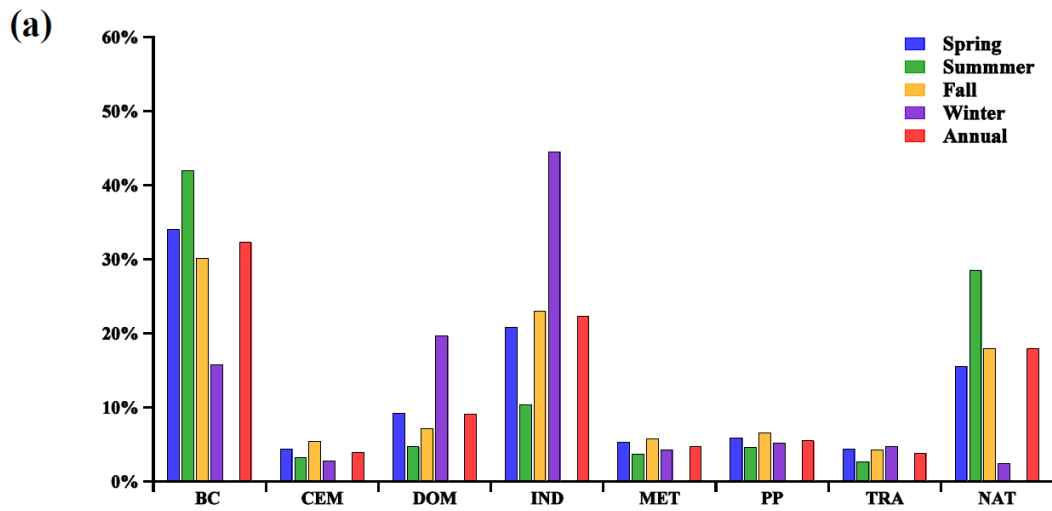


749

750 Figure 4 Source contributions to seasonal and annual averaged (a) GEM (b) GOM (c)

751

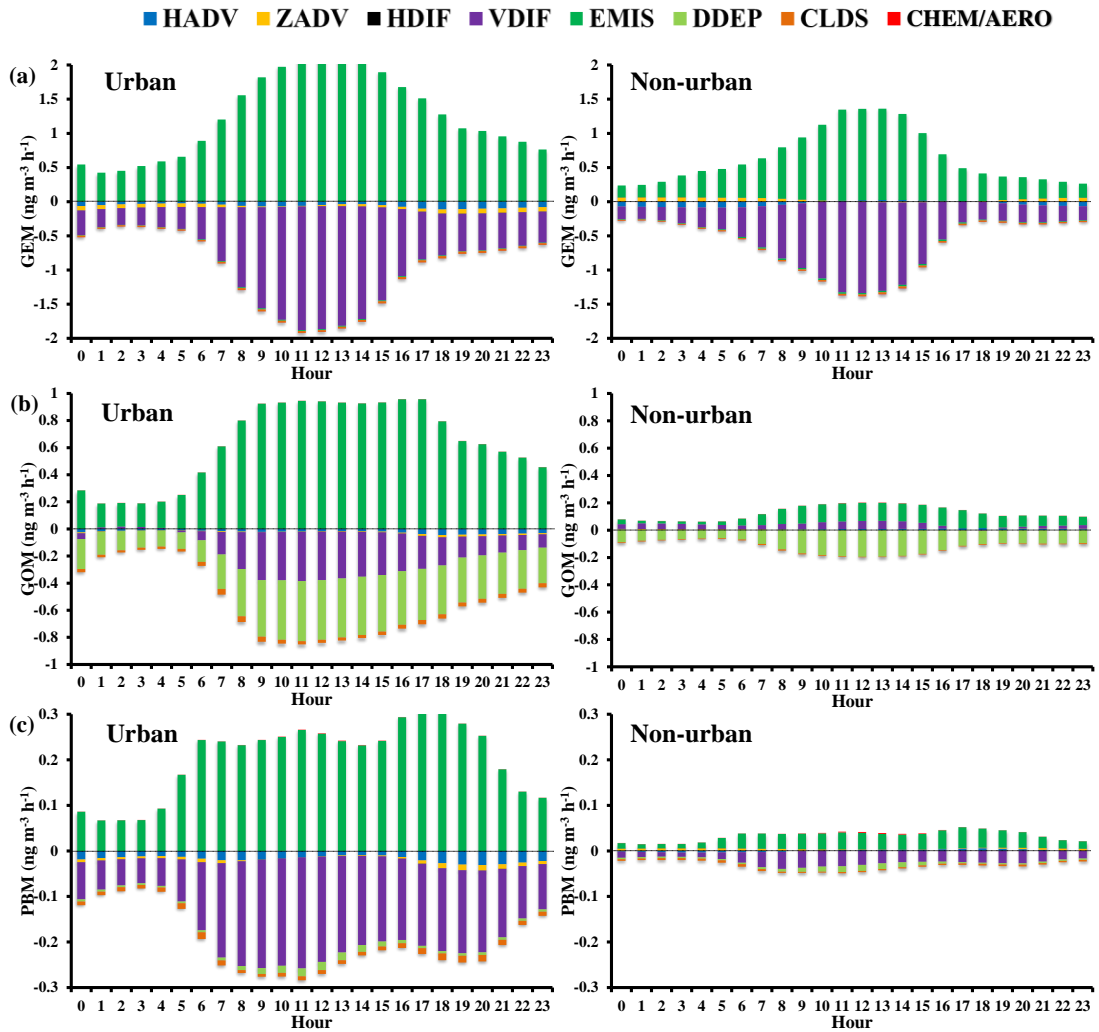
PBM concentration.



752

753 Figure 5 Source contributions to seasonal and annual mercury (a) wet and (b) dry
 754 deposition

755



756

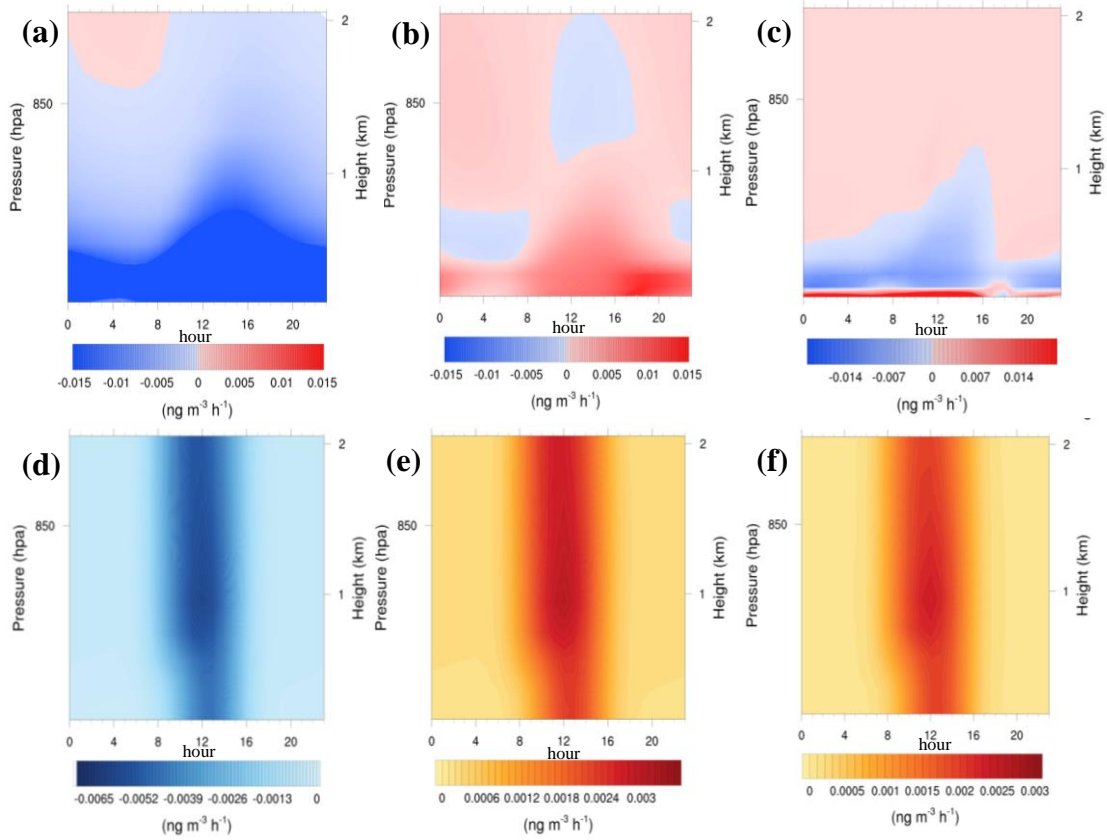
757 Figure 6 Diurnal variations of processes of (a) GEM, (b) GOM and (c) PBM in urban

758

and non-urban area.

759

760



761

762

Figure 7 Profile of the contribution of (a) HADV to GOM in urban area and (b)

763

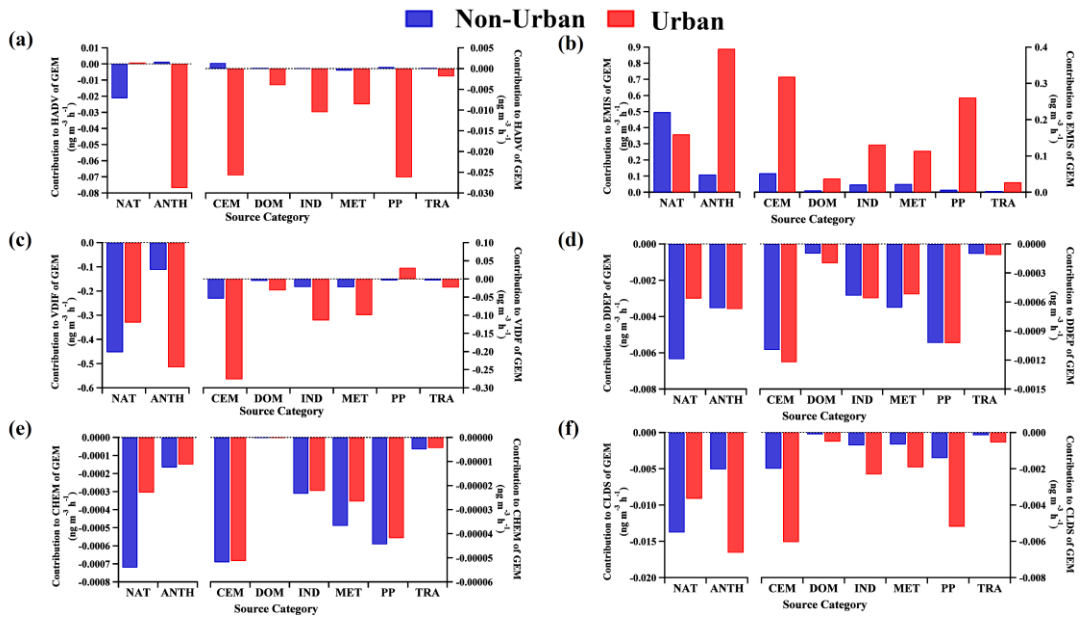
HADV to GOM, (c) VDIF to GOM, (d) CHEM to GEM, (e) CHEM to GOM, (f)

764

AERO to PBM in non-urban area.

765

766



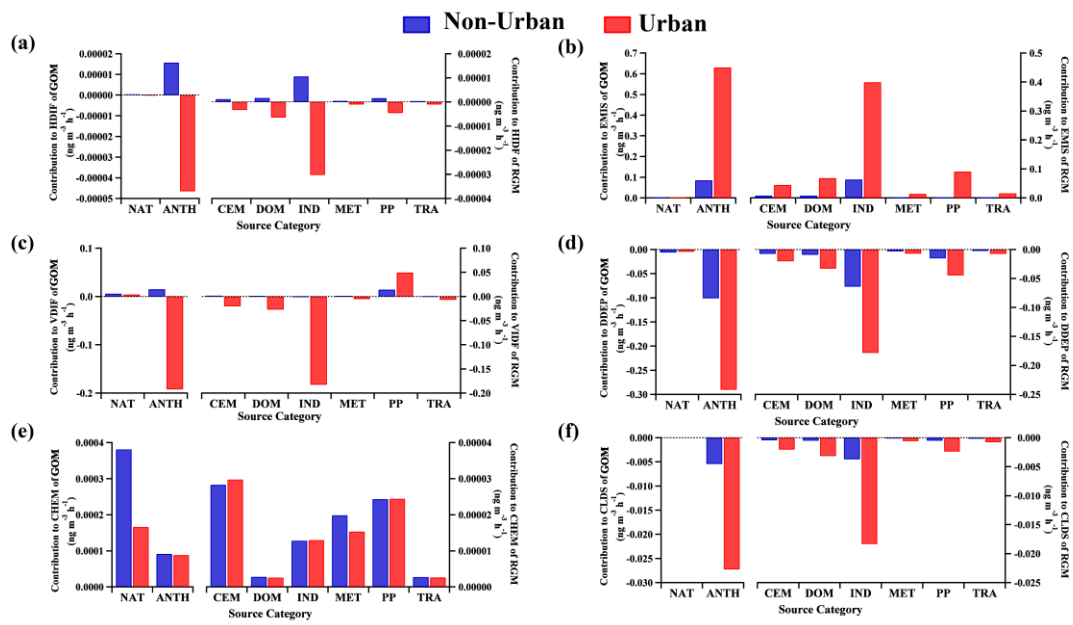
767

768 Figure 8 Impact of emission sources on (a) HADV, (b) EMIS, (c) VDIF, (d) DDEP, (e)

769

CHEM and (f) CLDS processes of GEM

770

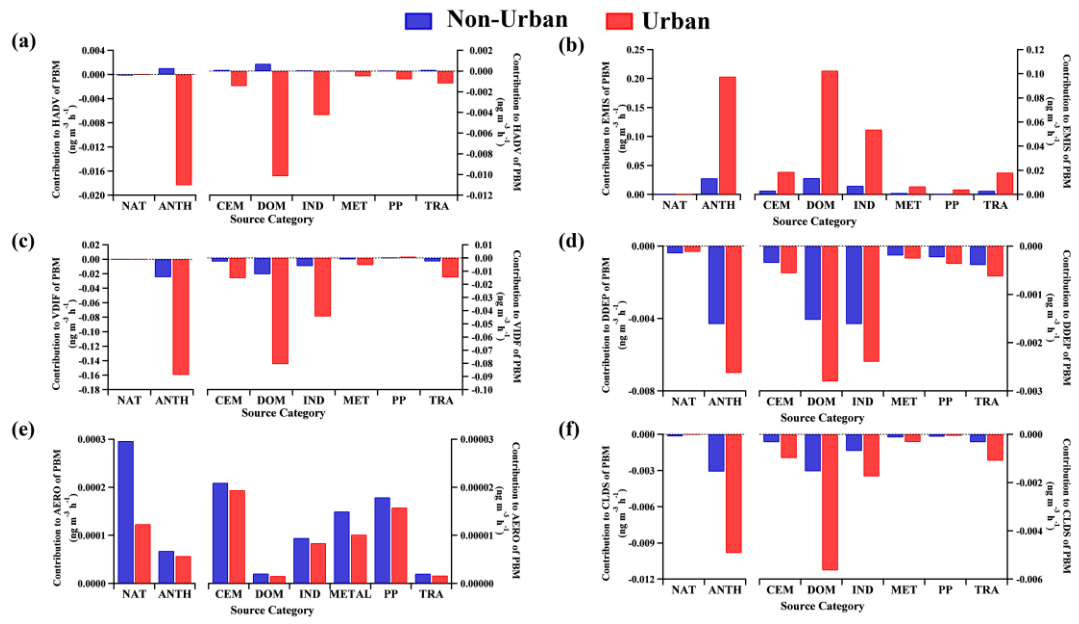


771

772 Figure 9 Impact of emission sources on (a) HADV, (b) EMIS, (c) VDIF, (d) DDEP, (e)

773

CHEM and (f) CLDS processes of GOM



774

775 Figure 10 Impact of emission sources on (a) HADV, (b) EMIS, (c) VDIF, (d) DDEP,

776

(e) AERO and (f) CLDS processes of PBM